Available online at www.sciencedirect.com
SCIENCE DIRECT®
Journal of Solid State Chemistry 178 (2005) 2128–2132
JOURNAL OF SOLID STATE CHEMISTRY
www.elsevier.com/locate/jssc

Preparation, structures, and band gaps of $RbInS_2$ and $RbInSe_2$

Fu Qiang Huang[a,c], Bin Deng[a], Donald E. Ellis[b], James A. Ibers[a,*]

[a]Department of Chemistry, Northwestern University, 2145 Sheridan Road, Evanston, Illinois 60208-3113, USA
[b]Department of Physics & Astronomy, Northwestern University, 2145 Sheridan Road, Evanston, Illinois 60208-3113, USA
[c]Shanghai Institute of Ceramics, Shanghai 200050, PR China

Received 4 February 2005; received in revised form 31 March 2005; accepted 6 April 2005

Abstract

The two compounds $RbInS_2$ and $RbInSe_2$ have been synthesized at 773 K by means of the reactive flux method. These isostructural compounds crystallize in space group $C2/c$ of the monoclinic system with 16 formula units in a cell at 153 K of dimensions $a = 11.0653(7)$ Å, $b = 11.0643(7)$ Å, $c = 15.5796(9)$ Å, and $\beta = 100.244(1)^\circ$ for $RbInS_2$, and $a = 11.477(3)$ Å, $b = 11.471(3)$ Å, $c = 16.186(6)$ Å, and $\beta = 100.16(2)^\circ$ for $RbInSe_2$. The In atoms are four-coordinated. The structure consists of two-dimensional $^2_\infty[In\,Q_2^-]$ (Q = S, Se) layers perpendicular to [001] separated from the Rb^+ cations. Adamantane-like In_4Q_{10} units are connected by common corners to form the layers. Band structure calculations indicate that these compounds are direct band-gap semiconductors with the smallest band gap at the Γ point. The calculated band gaps are 2.8 eV for $RbInS_2$ and 2.0 eV for $RbInSe_2$, values that are consistent with the colors of the compounds.

Keywords: Synthesis; Crystal structure; Band gaps; Chalcogenide; Indium

1. Introduction

The ternary chalcogenides $A/M/Q$ (where A = alkali metal; M = p-block metal; Q = S, Se, Te) have attracted much interest owing to their rich structural chemistry. When M = In, the structures vary widely as a function of composition. For example, the structure of $Rb_6In_2S_6$ [1] contains isolated $[In_2S_6]^{6-}$anions but the structure of $Rb_4In_2S_5$ [1] contains connected $[In_2S_6]$ units. The structure of Na_5InTe_4 [2] contains isolated $[InTe_4]$ tetrahedra, whereas that of $Na_5In_2Te_6$ [2] contains one-dimensional $^1_\infty[In_2Te_6^{5-}]$ chains formed by corner-sharing $[InTe_4]$ tetrahedra. The coordination number of the In center in chalcogenides also varies. It is often four ($LiInTe_2$ [3], $NaInTe_2$, $KInTe_2$ [4], and $KInS_2$, [5]), but six is also common ($NaInS_2$ and $NaInSe_2$ [6]). The composition and coordination versatility play important roles in the structural diversity of the $A/In/Q$ family.

For the $AInQ_2$ family there exist three common structural types. $NaInTe_2$ is isostructural with TlSe, crystallizing in space group $I4/mcm$ of the tetragonal system [4]. $NaInS_2$ exhibits the α-$NaFeO_2$ structure (space group $R\bar{3}m$ of the trigonal system) [6], which is an ordered structure of a rock salt derivative. These two structural types are usually high-pressure forms in the $AInQ_2$ system. The ambient-pressure forms of $KInS_2$ [5] and $KInSe_2$ [7] crystallize in space group $C2/c$ of the monoclinic system.

Here we provide details of the syntheses, structures, and electronic structures of $RbInS_2$ and $RbInSe_2$. Although the lattice constants for $RbInS_2$ have been determined in a powder X-ray diffraction study [8], insofar as we can determine full single-crystal structure determinations have not been reported for either of these compounds.

*Corresponding author. Fax: +1 847 491 2976.
E-mail address: ibers@chem.northwestern.edu (J.A. Ibers).

0022-4596/$ - see front matter © 2005 Elsevier Inc. All rights reserved.
doi:10.1016/j.jssc.2005.04.007

2. Experimental

2.1. Syntheses

The following reagents were used as obtained: Rb (Aldrich, 98 + %), In (Strem, 99.5%), S (Alfa Aesar, 99.5%), and Se (Alfa Aesar, 99.5%). Rb_2S_3 and Rb_2Se_3, the reactive fluxes [9] employed in the syntheses, were prepared by the stoichiometric reactions of the elements in liquid NH_3. Each compound was synthesized by the reaction of 1.0 mmol of In, 2.0 mmol of Se, and 0.5 mmol of Rb_2Q_3 (Q = S or Se). A reaction mixture was loaded into a fused-silica tube under an Ar atmosphere in a glove box. The tube was sealed under a 10^{-4} Torr atmosphere and then placed in a computer-controlled furnace. The sample was heated to 773 K in 10 h, kept at 773 K for 72 h, and then slowly cooled at 4 K/h to 293 K. The products were washed with de-ionized water and dried with methanol. Unoptimized yields of $RbInQ_2$ crystals were about 30%, based on In. No attempt was made to optimize yields. Other products were binary chalcogenide powders. Selected crystals, which were easily separated from the side products, were examined with an EDX-equipped Hitachi S-3500 SEM. The results were consistent with the stated compositions. $RbInS_2$ is pale brown whereas $RbInSe_2$ is red-yellow in color.

2.2. Crystallography

Single-crystal X-ray diffraction data were obtained with the use of graphite-monochromatized Mo$K\alpha$ radiation ($\lambda = 0.71073$ Å) at 153 K on a Bruker Smart-1000 CCD diffractometer [10]. The crystal-to-detector distance was 5.023 cm. Crystal decay was monitored by recollecting 50 initial frames at the end of data collection. Data were collected by a scan of 0.3° in ω in four groups of 606 frames at ϕ settings of 0°, 90°, 180°, and 270°. The exposure time was 15 s/frame. The collection of the intensity data was carried out with the program SMART [10]. Cell refinement and data reduction were carried out with the use of the program SAINT [10] and face-indexed absorption corrections were performed numerically with the use of the program XPREP [11]. Then the program SADABS [10] was employed to make incident beam and decay corrections.

The structures were solved with the direct methods program SHELXS and refined with the full-matrix least-squares program SHELXL of the SHELXTL suite of programs [11]. Each final refinement included anisotropic displacement parameters and a secondary extinction correction. The program STRUCTURE TIDY [12] was then employed to standardize the atomic coordinates. Additional crystallographic details are given in Table 1 and in Supplementary information. Table 2 presents selected metrical details.

Table 1
Crystal data[a] and structure refinements for $RbInS_2$ and $RbInSe_2$

Compound	$RbInS_2$	$RbInSe_2$
Formula weight	264.41	358.21
Space group	$C2/c$	$C2/c$
a (Å)	11.0653(7)	11.477(3)
b (Å)	11.0643(7)	11.471(3)
c (Å)	15.5796(9)	16.186(6)
β (°)	100.244(1)	100.16(2)
V (Å^3)	1877.0(2)	2097.5(1)
Z	16	16
ρ_c (g/cm^3)	3.743	4.537
μ (cm^{-1})	160.2	274.2
$R(F)$[b]	0.0252	0.0395
$R_w(F_o^2)$[c]	0.0663	0.1143

[a] For both structures $T = 153$ K and $\lambda = 0.71073$ Å.
[b] $R(F) = \Sigma||F_o| - |F_c||/\Sigma|F_o|$ for $F_o^2 > 2\sigma(F_o^2)$.
[c] $R_w(F_o^2) = \{\Sigma[w(F_o^2 - F_c^2)^2]/\Sigma wF_o^4\}^{1/2}$ for all data. $w^{-1} = \sigma^2(F_o^2) + (zP)^2$, where $P = (\mathrm{Max}(F_o^2, 0) + 2 \times F_c^2)/3$ and where $z = 0.03$ for $Q = S$ and 0.06 for Q = Se.

2.3. Electronic structure calculation

Electronic structures were calculated by the TB-LMTO program, which is a self-consistent, scalar relativistic linearized muffin-tin orbital program by Andersen and co-workers within the atomic sphere approximation (ASA) [13–15]. This method splits the crystal space into overlapping atomic spheres (Wigner–Seitz spheres). To achieve space filling with the ASA, nine empty spheres and eight empty spheres were introduced for $RbInS_2$ and $RbInSe_2$, respectively. The positions and radii of the empty spheres were calculated automatically. The radii for the Rb, In, S, and Se atoms were also determined automatically to provide overlaps of more than 16% for any two atom-centered spheres. The calculated radii were 4.23, 2.79, and 2.59 a.u. for Rb, In, and S in $RbInS_2$ and 4.43, 2.85, and 2.78 a.u. for Rb, In, and Se in $RbInSe_2$. In the present calculations, the von Barth-Hedin exchange-correlation potential was used within the local density approximation (LDA) [16]. All k-space integrations were performed with the tetrahedron method with the use of 242 k points [17,18]. The basis sets consisted of the valence 5s electrons for Rb; 5s and 5p electrons for In; 3s and 3p electrons for S; 4s and 4p electrons for Se; and 1s states for empty spheres. The 5p and 5d electrons for Rb, 4d electrons for In, 3d electrons for S, 4d electrons for Se, and p–d states for empty spheres were downfolded by means of the technique described by Löwdin [19].

3. Results and discussion

$RbInS_2$ and $RbInSe_2$ have been synthesized in about 30% yield by the reactions of the elements in Rb_2S_3 and

Table 2
Selected bond distances (Å) and bond angles (deg) for $RbInQ_2$

Distance or angle	$Q = S$	$Q = Se$	Distance or angle	$Q = S$	$Q = Se$
In1–Q3	2.452(1)	2.567(1)	In1–Q4	2.455(1)	2.567(1)
In1–Q1	2.456(1)	2.566(1)	In1–Q2	2.458(1)	2.573(1)
In2–Q1	2.453(1)	2.563(1)	In2–Q3	2.456(1)	2.565(1)
In2–Q5	2.456(1)	2.565(1)	In2–Q2	2.457(1)	2.573(1)
Rb1–Q1	3.312(1)	3.447(2)	Rb1–Q2	3.330(1)	3.455(2)
Rb1–Q3	3.482(1)	3.598(2)	Rb1–Q4	3.4818(5)	3.600(1)
Rb1–Q3	3.483(1)	3.600(2)	Rb1–Q5	3.4828(5)	3.600(1)
Rb2–Q1	3.312(1)	3.402(1)	Rb2–Q2	3.330(1)	3.411(1)
Rb2–Q5	3.401(1)	3.523(2)	Rb2–Q3	3.402(1)	3.519(1)
Rb2–Q4	3.403(1)	3.518(1)	Rb2–Q3	3.405(1)	3.524(1)
Q3–In1–Q4	111.17(3)	112.14(3)	Q3–In1–Q1	111.74(4)	112.20(4)
Q4–In1–Q1	111.81(3)	112.17(4)	Q3–In1–Q2	108.19(4)	107.71(4)
Q4–In1–Q2	108.12(4)	107.65(4)	Q1–In1–Q2	105.52(4)	104.47(4)
Q1–In2–Q3	111.77(4)	112.17(4)	Q1–In2–Q5	111.70(3)	112.15(4)
Q3–In2–Q5	111.23(3)	112.29(3)	Q1–In2–Q2	105.67(4)	104.15(4)
Q3–In2–Q2	108.08(4)	107.70(4)	Q5–In2–Q2	108.09(4)	107.85(4)

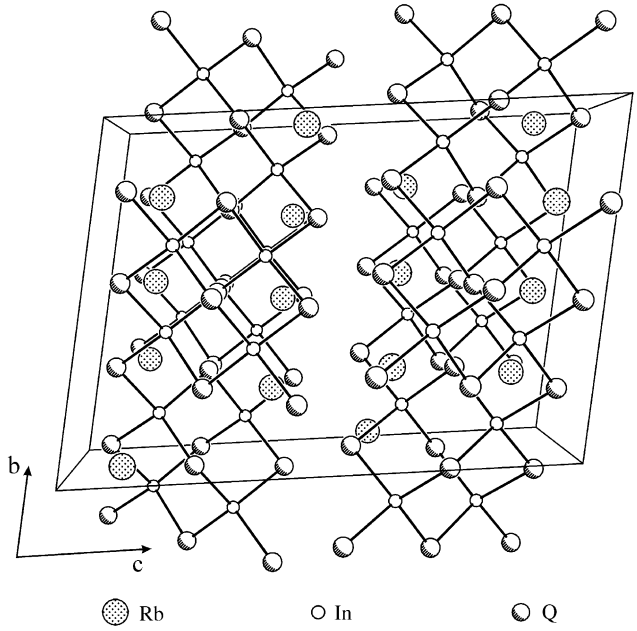

Fig. 1. Unit cell of $RbInQ_2$ ($Q = S$, Se) viewed down [100].

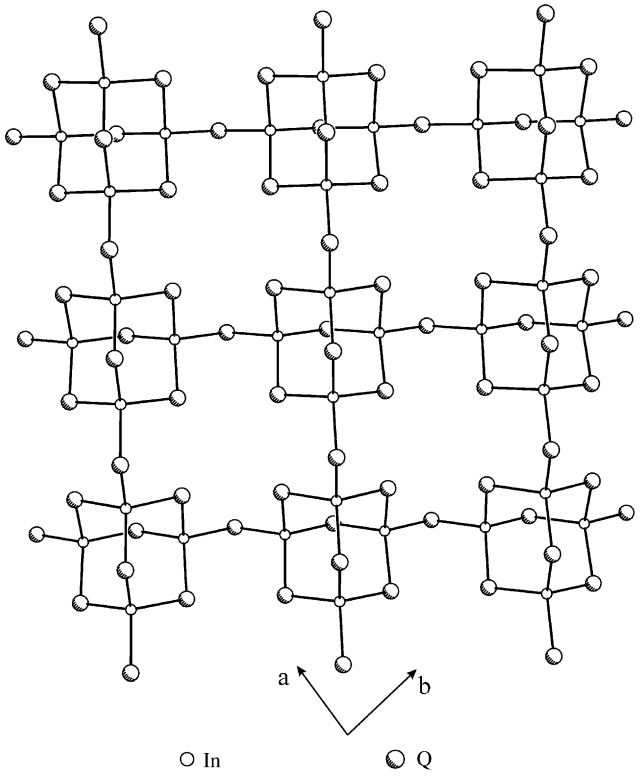

Fig. 2. The two-dimensional $^2_\infty[InQ_2^-]$ layer viewed down [001].

Rb_2Se_3 fluxes at 773 K. These compounds are stable in air for at least 1 week. After about 2 months crystals degrade into gray powders.

The isostructural compounds $RbInS_2$ and $RbInSe_2$ crystallize with 16 formulas in space group $C2/c$ of the monoclinic system, and are isostructural with their K analogues [5,7]. Fig. 1 shows a view of the crystal structure down the [100] direction. The structure consists of two-dimensional $^2_\infty[InQ_2^-]$ layers separated by Rb^+ cations. The structure of the $^2_\infty[InQ_2^-]$ layer is shown in Fig. 2. These layers stack perpendicular to the [001] direction. Each layer is related to the ones above and below it by a two-fold rotation. A given layer consists of corner-sharing adamantane-like $[In_4Q_{10}]$ units comprising four corner-sharing $[InQ_4]$ tetrahedra, as shown in Fig. 3 for $Q = S$. It was noted recently [16] that highly ordered crystals of $RbInS_2$ can be prepared easily. Consistent with this, the displacement ellipsoids shown in Fig. 3 provide no indication of disorder arising from stacking faults of the $^2_\infty[InS_2^-]$ layers.

In $RbInS_2$, each Rb^+ cation is surrounded by eight S atoms in an irregular polyhedron, with six shorter and

two longer Rb–S interactions. The shorter distances range from 3.312 (1) to 3.4828 (5) Å, comparable to those of 3.247 (2) to 3.7951(4) Å in $RbNd_2CuS_4$ [17]. The In–S distances range from 2.452 (1) to 2.458 (1) Å, which are also comparable to those of 2.421(3) to 2.482 (3) Å in $KInS_2$ [5]. The S–In–S bond angles in $RbInS_2$ range from 105.52(4)° to 111.81(3)°, close to those of 105.1(1)° to 113.3(1)° in $KInS_2$ [5]. In $RbInSe_2$, each Rb^+ cation has six shorter and two longer Rb–Se interactions. The shorter Rb–Se distances range from 3.402(1) to 3.600(2) Å, which are consistent with those of 3.3814(9) to 3.4599(8) Å in $RbLnSe_2$ (Ln = La, Ce, Pr, Nd, Sm, Gd, Tb, Ho, Er, Lu) [18]. The In–Se distances range from 2.563(1) to 2.573(1) Å, which are comparable to those of 2.537(2) to 2.856(2) Å in Pr_3InSe_6 [19]. The $InSe_4$ tetrahedra are somewhat more distorted than the InS_4 tetrahedra, with the Se–In–Se bond angles ranging from 104.15(4)° to 112.29(3)°.

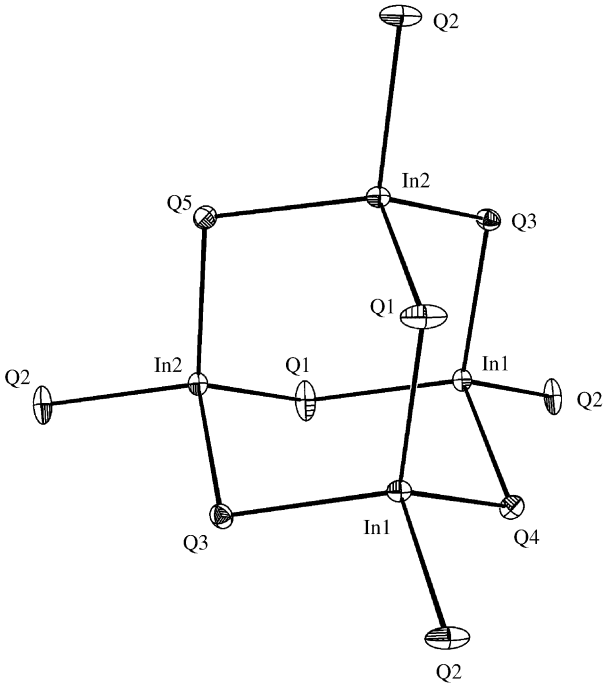

Fig. 3. Adamantane-like $[In_4Q_{10}]$ units in $RbInS_2$.

Fig. 4 shows the total and partial densities of states (DOS) of $RbInS_2$. The Rb electrons make almost no contribution around the Fermi level. Therefore, the electronic properties are mainly determined by the $[InS_2^-]$ layers. As indicated in Fig. 4, most of contributions in the conduction band are from In (5*s*) and In (5*p*) electrons. In the valence band, S (3*p*) electrons are hybridized with In (5*s*) and In (5*p*) electrons to form In–S bonds. The In (5*s*) electrons are mainly localized in the region from −5 to −4 eV, whereas the In (5*p*) electrons are mainly localized in the region from −2.5 eV to the Fermi level. The band structure of $RbInS_2$ is shown in Fig. 5. The bands near the Fermi level are very flat with little dispersion, consistent with the localization of In (5*s*) and In (5*p*) electrons in the valence band. The valence band maximum and conduction band minimum are both located at the Γ point. Therefore, $RbInS_2$ is a

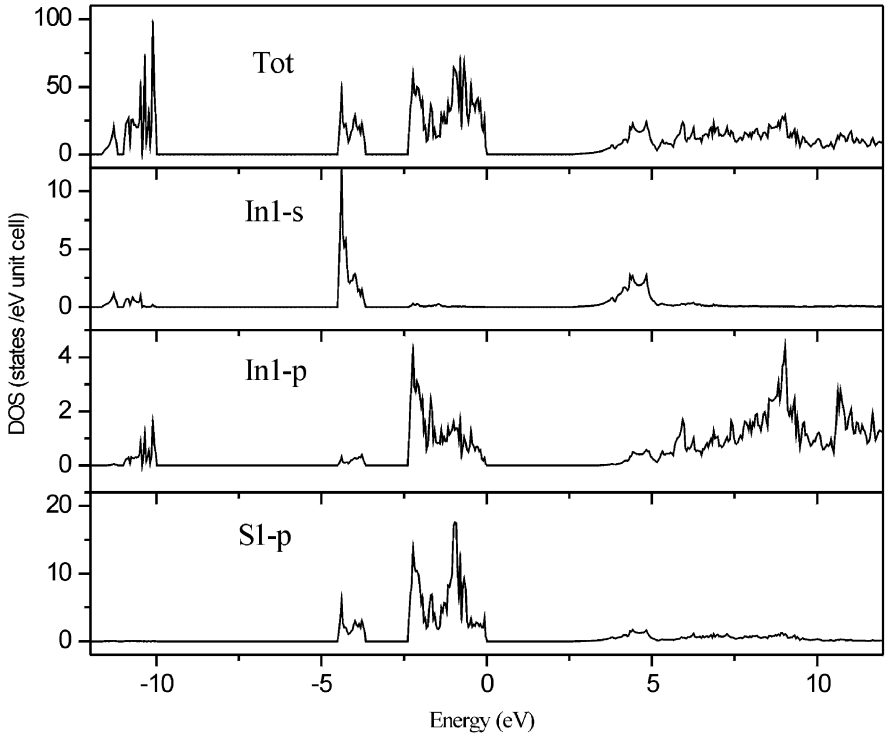

Fig. 4. Total and partial DOS of $RbInS_2$.

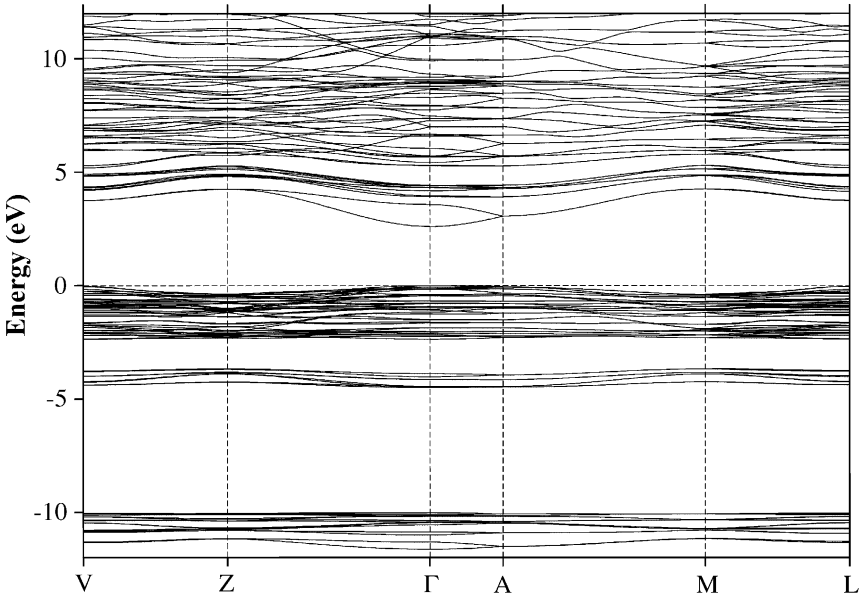

Fig. 5. Band structure of $RbInS_2$.

direct band-gap semiconductor. The DOS and band structure of $RbInSe_2$ (not shown) are similar to those of $RbInS_2$. However, the energy level of the S (3*p*) orbitals is lower than that of the Se (4*p*) orbitals; this leads to a higher energy level of Se for the valence band of $RbInSe_2$ and thus to a smaller band gap. From the band structures, the direct band gaps of $RbInS_2$ and $RbInSe_2$ are 2.8 and 2.0 eV, respectively, consistent with their respective colors of pale brown and red-yellow.

Supplementary information

The crystallographic files in cif format for $RbInS_2$ and $RbInSe_2$ have been deposited as CSD numbers 415086 and 415087, respectively. The data may be obtained free of charge by contacting FIZ Karlsruhe at +49 7247 808 666 (fax) or crysdata@fiz-karlsruhe.de (email)

Acknowledgments

This research was supported in part by the US National Science Foundation under Grant DMR00-96676. FQH also acknowledges support from the NSF of China Grant B010504-20471068. Use was made of the MRL Central Facilities supported by the US National Science Foundation at the Materials Research Center of Northwestern University under Grant DMR00-76097.

References

[1] H.-J. Deiseroth, Z. Naturforsch. B: Anorg. Chem. Org. Chem. 35 (1980) 953–958.
[2] B. Eisenmann, A. Hofmann, R. Zagler, Z. Naturforsch. B: Chem. Sci. 45 (1990) 8–14.
[3] W. Hönle, G. Kühn, H. Neumann, Z. Anorg. Allg. Chem. 532 (1986) 150–156.
[4] E.R. Franke, H. Schäfer, Z. Naturforsch. B: Chem. Sci. 27 (1972) 1308–1315.
[5] C.K. Lowe-Ma, D.O. Kipp, T.A. Vanderah, J. Solid State Chem. 92 (1991) 520–530.
[6] R. Hoppe, W. Lidecke, F.-C. Frorath, Z. Anorg. Allg. Chem. 309 (1961) 49–54.
[7] P. Wang, X.-Y. Huang, Y.-L. Liu, J. Li, H.-Y. Guo, Huaxue Xuebao 58 (2000) 1005–1008.
[8] H. Schubert, R. Hoppe, Z. Naturforsch. B: Anorg. Chem. Org. Chem. Biochem. Biophys. Biol. 25 (1970) 886–887.
[9] S.A. Sunshine, D. Kang, J.A. Ibers, J. Am. Chem. Soc. 109 (1987) 6202–6204.
[10] Bruker, SMART Version 5.054 Data Collection and SAINT-Plus Version 6.45a Data Processing Software for the SMART System, 2003 (Bruker Analytical X-ray Instruments, Inc., Madison, WI, USA).
[11] G.M. Sheldrick, SHELXTL Version 6.14, 2003 (Bruker Analytical X-ray Instruments, Inc., Madison, WI, USA).
[12] L.M. Gelato, E. Parthé, J. Appl. Crystallogr. 20 (1987) 139–143.
[13] O.K. Andersen, Phys. Rev. B 12 (1975) 3060–3083.
[14] O.K. Andersen, O. Jepsen, Phys. Rev. Lett. 53 (1984) 2571–2574.
[15] O. Jepsen, O.K. Andersen, Z. Phys. B: Condens. Matter 97 (1995) 35–47.
[16] L. Kienle, V. Duppel, A. Simon, M. Schlosser, O. Jarchow, J. Solid State Chem. 177 (2004) 6–16.
[17] F.Q. Huang, J.A. Ibers, J. Solid State Chem. 158 (2001) 299–306.
[18] B. Deng, D.E. Ellis, J.A. Ibers, Inorg. Chem. 41 (2002) 5716–5720.
[19] L.E. Aleandri, J.A. Ibers, J. Solid State Chem. 79 (1989) 107–111.